Draft version May 6, 2023
Typeset using LaTeX **twocolumn** style in AASTeX631

Fate of Solar System-Like Stars in MW-M31 Merger

Ansh R. Gupta [1]

[1] *Steward Observatory, University of Arizona, 933 N Cherry Avenue, Tucson, AZ 85721, USA*

(Dated: April 5, 2023)

ABSTRACT

The Milky Way and M31 are currently on a collision course and are expected to merge in ∼6 billion years. Understanding how stellar populations will migrate and change throughout this event yields tools to analyze galaxy evolution and produces statistical predictions about the eventual fate of the Solar System. In this work, I explore the distribution of Sun-like stars in M31 before, during, and after the merger to determine the movement and fate of this population using simulation data from van der Marel et al. (2012). A visualization movie showing the positions of these particles over time demonstrates the disruption of their orbits during passes between the Milky Way and M31. An additional video sequence of histograms showing the particle radii at each time step aids in the qualitative analysis of these same findings. Moreover, a plot of the maximum, minimum, and median radii of selected particles over time shows that significant radial migration occurs around 6 Gyr from today but that all system particles remain within ∼75 kpc of the merger remnant. These results indicate that although Sun-like stars in M31 remain gravitationally bound to the system, they can migrate a significant distance outward and are roughly spherically distributed around the merger remnant after 12 Gyr.

Keywords: Local Group — Merger remnant — Stellar disk — Stellar bulge — Dark Matter Halo

1. INTRODUCTION

The Local Group (LG) is a group of galaxies dominated in mass by the Milky Way (MW) and Andromeda galaxy (M31). The LG's third most massive object, the Triangulum galaxy (M33), is a satellite of M31 (Sparke & Gallagher 2007). Current estimates indicate that the MW and M31 will merge in approximately 5.86 Gyr; many stars will remain within the merger remnant, which consists of the bulk of the stars, gas, and dark matter that coalesce into a single galaxy following the merging event (van der Marel et al. 2012). The expected morphology of the MW and M31 during and after the merger has far-reaching consequences. Components of spiral galaxies include the stellar disk, a relatively thin region of space along a galactic plane including significant amounts of dust, gas, and stars; the stellar bulge, a more spherical, compact region at the center of spiral galaxies; and a dark matter halo, which is a spheroidal distribution of matter containing the majority of the mass content in most galaxies (Belokurov et al. 2018). Studying the evolution of these galaxy components can yield insight into how interacting galaxies grow and change over time (Torrey et al. 2012), give information about the migration of stars throughout galaxies over time (Roškar et al. 2012), and produce statistical predictions about the long-term trajectories of the Sun and similar stars (van der Marel et al. 2012). Here, I create a visualization of the eventual fate of a specific subset of bodies within M31. Specifically, I determine whether stars at a similar distance from the M31 galaxy core as the Sun's galactocentric distance remain within the merger remnant, are ejected, or are captured by M33. To aid in the visualization of these results, a movie of the merger event highlighting the selected particles was created. I also create a video series of histograms showcasing the distribution of Sun-like particle radii from the M31 COM over time. Moreover, I determine the maximum, minimum, and median radii of these Sun-like particles over time and produce a plot to showcase the range in radii before and after the merger.

Selecting specific stellar populations and determining their outcomes following a merger is a powerful method to probe how the composition and morphology of interacting galaxies change over time (van der Marel et al. 2012). While I aim to select only Sun-like stars in this work, these methods can be modified to probe the general kinematics of stars stars in a galactic disk, bulge,

or halo. The varying interactions of these galaxy components may help predict the long term evolution and growth of merging galaxies (Dubinski et al. 1996). Visualizations can help display patterns that might be difficult to notice in data, contributing to the maturity and success of a variety of science projects (Pomarède et al. 2017). They also serve as a vital tool for public outreach, promoting education, scientific literacy, and public engagement with the research process (Rector et al. 2017). Methods to understand the long term evolution of galaxies by component are necessary to make astrophysical predictions about the past and future (Sohn et al. 2012). Specifically, galaxy evolution is the set of processes through which galaxies formed, generating specific structures, and which cause changes in kinematics and morphology over time (Sparke & Gallagher 2007). Indeed, the definition of a galaxy is a gravitationally bound collection of stars, gas, dust, and dark matter (Willman & Strader 2012). Investigating the mechanisms which cause these constituents to form structures and evolve is a major area of study in astronomy. Knowledge of the evolution of Sun-like stars in multiple galaxies will contribute to this field of interest.

Current state-of-the-art simulations suggest that the majority of Sun-like stars in the Milky Way will remain within the merger remnant. However, analysis reveals that these objects will be distributed much more evenly throughout the remnant. van der Marel et al. (2012) use a canonical N-body simulation of the merger to show that a large majority of objects in a Sun-like orbit within the MW ($> 85\%$) migrate outwards following the merger, but most remain within ~ 50 kpc. A minority ($< 0.1\%$) are ejected out to a large radius (> 100 kpc), but all candidates in the simulation remained gravitationally bound to the system. Although approximately 20% of the candidates in the simulation pass through M33, none are accreted by the galaxy. Many of the selected stars are dislodged into "stellar streams", long tails of stars cast out during the merging process. Several stellar streams caused by the tidal disruption of dwarf galaxies have been discovered in the MW halo (Belokurov et al. 2006, and references therein). Martin et al. (2014) show that some streams caused by the tidal disruption of dwarf galaxies show a strong radial distance gradient, which is consistent with the low proportion of highly distant Sun-like stars from the merger simulation. Snapshots of the simulation from van der Marel et al. (2012) are shown in Figure 1, which visually summarize the possible fates of Sun-like stars and display the structure of the stellar streams.

Although previous work investigates the future of MW Sun-like stars, the fate of such objects in the M31 disk has not yet been studied. Furthermore, it's not clear whether analogous systems in M33 are captured in tidal tails, accreted by the merger remnant, remain part of M33, or are otherwise ejected. Furthermore, previous simulations have not included other LG galaxies, such as the Large and Small Magellanic Clouds (Dubinski et al. 1996)(Cox & Loeb 2008)(van der Marel et al. 2012). An open question remains as to whether these other galaxies may have an affect on the merger, whether Sun-like stars will pass through them, and whether they may be disrupted by or impact the MW before the merger takes place. As the proper motions of other LG satellite galaxies have been better constrained, including them in future N-body simulations is a topic of interest (van der Marel 2015).

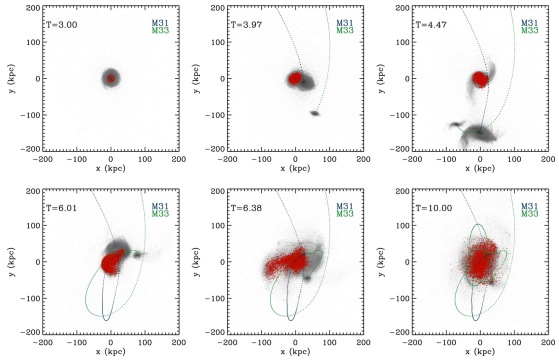

Figure 1. Individual frames from an N-body simulation of the MW-M31 merger, projected onto the galactocentric plane with the origin at the MW center of mass. The time of each snapshot is shown in the top left, with dotted lines indicating galaxy orbital paths. Sun-like stars are shown in red. Most of the selected stars migrate outwards, some are cast into stellar streams, and a small fraction are ejected far away. All objects remain gravitationally bound to the system. Figure adapted from van der Marel et al. (2012).

2. THIS PROJECT

In this work, I select sun-like particles in the disk of M31 and M33 and track their motions over the course of the merging event using N-body simulation data supplied from van der Marel et al. (2012). I create a movie visualization of the merger event to demonstrate the bulk migration of these particles over time. Moreover, I make histogram plots at each simulation snapshot showing the distribution of particle positions and form them into another video sequence. Finally, I produce a plot displaying the maximum, minimum, and median particle radii over time. Sun-like stars are selected to have a similar distance from the M31 galactic center as the Sun's distance to the center of the MW (~ 8.29 kpc), a maximum out-of-plane velocity of 100 kms^{-1}, and a

circular velocity within 10% of the circular speed computed using the enclosed mass at each particle's radius.

This study addresses the question of where a specific subset of stars will reside after the MW-M31 collision. Specifically, this study demonstrates the relative fractions of M31 Sun-like stars that remain in the remnant, are ejected out of the LG, and are cast into tidal tails.

Knowledge of the future kinematics of this group of objects cam help determine the eventual fate of Sun-like particles in the disk of M31 following the merger and contribute to the understanding of how specific galactic disk components evolve over time following major merger events. These visualizations are qualitatively used to examine the morphological distribution of the selected objects following the merger, which visually displays the possible and most likely far-future orbits of Sun-like stars in M31 and M33. The numerical plot showing the maximum radius of the selected particles over time places an upper bound on the most distant particles and reveals whether this class of objects are likely to be ejected from the system and if they remain gravitationally bound to the merger remnant.

3. METHODOLOGY

Simulation data is supplied from van der Marel et al. (2012), in which an N-body simulation is used to determine the outcome and properties of the MW-M31 merger in the next 10 Gyr from the current time. An N-body simulation is one in which the positions of a number of particles over time are directly calculated using numerical integration considering the mutual forces between each each pair of particles. Each particle represents a specified mass of stars or dark matter. Gas and dust, which contribute only slightly to the overall mass of the galaxy, are neglected. van der Marel et al. (2012) use canonical initial conditions, those which are approximately in the middle of the range constrained by previous works. Furthermore, a Monte Carlo approach is used to quantify the effects of varying these parameters within these allowed ranges.

Sun-like particles are selected by applying a series of filters to the total sample of stars from the simulation. First, the selection is limited to particles within 10% of the Sun's galactocentric distance. Then, the circular velocity of each particle is computed, and only those with circular speeds within 10% of those computed using the enclosed galaxy mass are retained. Finally, the out-of-plane velocities of each particle are capped at 100 kms^{-1}. All objects that meet these criteria form the set of Sun-like particles used for the analysis. Plots are made showing the positions of this group of objects within the disk of M31 and M33 at each snapshot of the N-body simulation, and are stitched together into a movie to complete the final movie visualization. The first frame of the visualization is shown in Figure 2, with all particles that satisfy the listed criteria marked in a different color. 2797 particles are selected in M31 and 799 are selected in M33.

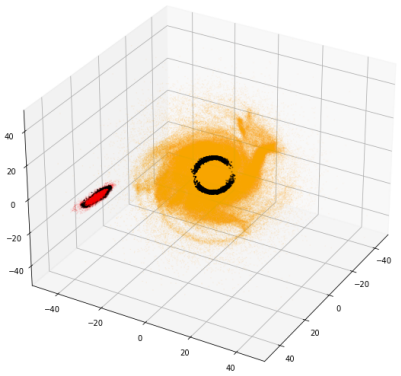

Figure 2. Example frame produced using Matplotlib showing the first frame of the visualization, with disk particles of M31 (orange) and M33 (red) shown. The visualization highlights Sun-like particles of M31 and M33 in black. The selected particles form an annulus around each galaxy since they are selected to be near the Sun galactocentric distance from their respective centers of mass. This selection is further filtered by setting a maximum out-of-plane velocity and requiring a circular speed close to that calculated from the enclosed mass at each radius. Simulation data taken from van der Marel et al. (2012).

To select Sun-like particles in M31 and M33 and produce visualizations tracking their orbital evolution, a few specific codes are created. An existing code uses iterative spheres of shrinking volume to calculate the center of mass (COM) of each galaxy to avoid contamination from ejected stars. Using these COM coordinates, the distance of each galaxy particle from its corresponding center is determined. A new code is created to determine the circular speed of particles by determining the tangential component of their overall velocity. This is accomplished by using a method to rotate the plane of a given galaxy such that its total angular momentum vector points along a specific axis. The perpendicular components of the velocity were then analyzed to give the circular speed. Specifically, the disk is rotated such that the angular momentum vector lies along the z-axis, meaning that the circular speed is determined as

$$v_{circ} = \sqrt{{v_x}^2 + {v_y}^2} \quad (1)$$

Using the determined radii and circular speeds, another code selects particles that match the Sun's distance from the galactic center within 10%. Then, the expected circular velocity at the selected radius values are computed using the total enclosed mass of the host galaxy. The theoretical circular speed of a particle at radius r with enclosed mass M_{enc} is

$$v_{circ} = \sqrt{\frac{GM_{enc}}{r}} \quad (2)$$

The particles are only retained if the measured v_{circ} is within 10% of the calculated value. At this time, the time-evolution of the Sun's orbit through the MW disk in the z-axis direction is not well constrained; instead, candidate Sun-like particles will be filtered by limiting their z-axis velocities to $100 kms^{-1}$ to exclude objects moving with significant out-of-plane velocity, which is within an order of magnitude as the limit used in van der Marel et al. (2012). The cutoff used in this work is higher than the previously used $30 kms^{-1}$ limit due to the latter overly restricting the available sample of Sun-like particles. Using the Python software Matplotlib, all particles are plotted, with the Sun-like stars assigned a separate color. The visualization proceeds centered on the M31 COM. These frames are stitched together into a movie using Adobe Premiere. Again using Matplotlib, a histogram with fixed bin size and axes limits is generated at each time step in the simulation, and these plots are sequenced into a second video. Finally, the maximum, minimum, and median Sun-like particle radius at each snapshot number are determined and plotted as a function of time.

The visualizations produced directly show where Sun-like stars in M31 and M33 are located over time. Qualitatively, these movies show how these objects migrate radially throughout the disk before the merger. The movie shows some stars disrupted as the galaxies interact, while the histogram video qualitatively displays this information. Additionally, the maximum radius plot gives information about the furthest of these objects, and whether they remain bound to the system. All of these visualizations yield information about the long term fate of the selected systems.

M31 is of comparable size to the MW, so one may expect that the trajectories of Sun-like stars are similar for both galaxies. One significant difference is that the M31 spin axis is nearly perpendicular to the orbital plane of the MW and M31, which also roughly defines the plane of the collision (van der Marel et al. 2012). This is in contrast to the MW, which has a closer orbital alignment. These differences may cause the dynamics of M31 Sun-like stars to differ from those of the MW, as stars off-axis from the collision may be more significantly disrupted. Also, as M33 is a satellite galaxy of M31, ejected stars may have a greater probability of being captured by it. However, overall, it seems reasonable to assume that the outcomes of these stars will be similar to those in the MW due to the similarities of the two galaxies.

4. RESULTS

The completed movie visualization is fixed on the center of mass frame of M31. As shown in Figure 2, the Sun-like particles begin in small annuli around M31 and M33, as defined by the selection criteria. As the simulation advances, some particles initially migrate out due to the kinematics of the system. However, before the first pass between the MW and M31, the selected particles all remain within the disk of their respective galaxies. After each pass of the two galaxies, Sun-like stars in M31 are disrupted to a greater extent. When the galaxies finally merge, these stars are distributed spherically throughout the remnant, but it can be seen that they remain gravitationally bound. Figure 3 shows the final frame of the simulation, encapsulating the much wider distribution of stars than from the initial conditions. The visualization displays a number of systems streaming away from and then returning to the remnant, giving a haunting image of the potential future fates of these systems.

Figure 4 shows the histogram of the galactocentric radii of Sun-like stars in M31 from the final snapshot in the simulation. Compared to narrow distribution of particle radii initially selected, these particles have experienced a significant radial migration. Still, most particles remain within 40 kpc of the merger remnant center of mass at the end compared to all particles starting off within 10 kpc. Within just a few billion years, the particles spread out and fill a distribution ranging up to 20 kpc. Because the MW is still very distant to M31 at this point, this demonstrates how the internal kinematics of the galaxy can carry Sun-like stars throughout the disk before the merger. As can be seen in Figure 4, the distribution of particles after the merger is significantly different than at the start of the simulation, showing how significantly the morphology of M31 is altered by the event.

In order to determine whether any particles are completely ejected from the system, the maximum radii of all Sun-like particles at each snapshot number of the simulation are found. In addition, the minimum and median particle radii are computed, and all three quantities are plotted in Figure 5. Because the maximum radius

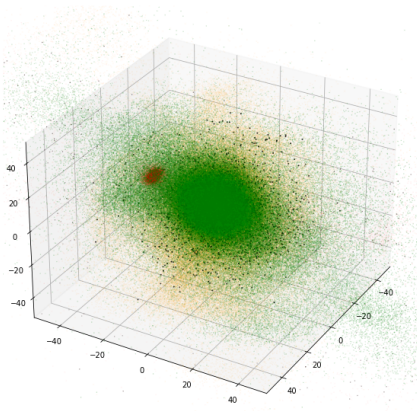

Figure 3. Final frame, snap number 800, from the galaxy merger visualization. MW particles are in green, M31 particles are in orange, and M33 particles are in red. Additionally, Sun-like stars from M31 and M33 are shown in black. Arbitrary axis units are in kpc. As shown in Figure 2, these particles initially started off in relatively well-defined annuli around their host but end up scattered throughout the merger remnant. It can be seen that Sun-like stars end up at a variety of radii distributed spherically, with the video showing how the first and especially the second pass influence the orbital characteristics of these stars. The full visualization can be found at the following YouTube link: https://www.youtube.com/watch?v=NOZLI3LgNMw. Simulation data taken from van der Marel et al. (2012).

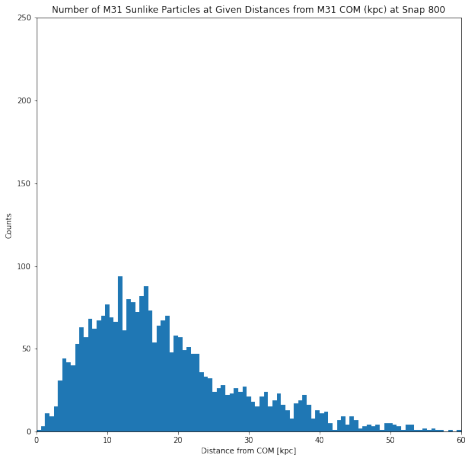

Figure 4. Histogram showing the distribution of M31 sun-like particle radii at the end of the simulation. The distance of particles from the M31 COM in kpc is plotted on the x-axis, with the number of particles within each bin on the y-axis. This is the final frame in a video showing how the distribution in the radii changes over time. As viewed alongside the full visualization movie, the histogram experiences significant shifts when the MW and M31 have near approaches and when they finally merge. This is a qualitative aid to Figure 3, and also shows that although some particles are expelled relatively far from the system, the most distant outliers have radii only a few times greater than the majority of particles. The full histogram series video can be found at the following YouTube link: https://www.youtube.com/watch?v=BiuS-Li1TUg.

seems relatively stable following the merger at ~ 6 Gyr, it is reasonable to conclude that none of the selected Sun-like particles from the simulation are ejected from the system. If any particle were to escape, the radius would grow without bound. Instead, this plot indicates that although the selected stars can migrate throughout the final merger remnant, they remain firmly within the system for the foreseeable future despite the turbulent nature of the collision.

5. DISCUSSION

The results of Figures 3 and 4 qualitatively and quantitatively are similar to the results from previous literature for MW Sun-like particles, but there appear to be some key differences. Specifically, the distribution of the radii of these particles in M31 at the end of the simulation, for example as shown in Figure 4, appears to be broader and centered at a higher average distance than Sun-like MW particles, as shown in Figure 8 of van der Marel et al. (2012). This may reinforce the idea that the nearly face-on inclination of M31 relative to the orbital plane of the collision causes many of these stars to be dislodged to a greater extent, in line with the hypothesis presented in the Methodology section.

However, these results could also be caused by a few procedural differences. For example, van der Marel et al. (2012) select Sun-like particles to have a maximum out-of-plane velocity of 30 kms^{-1}, whereas a number of 100 kms^{-1} is used in this work. Because of the less strict criteria employed here, a greater fraction of particles with more turbulent kinematics may have been selected in comparison. In addition, many fewer particles (2797 for M31 and 799 for M33) are used in this analysis, so the bin size of the generated histograms differs from that in the previous work.

Figure 5 demonstrates that none of the systems in consideration are ejected from the system. Because the radius of the most distant particles stays roughly constant following the merger, it can be concluded that all of the Sun-like stars remain gravitationally bound. This result agrees with the findings for the corresponding systems in the MW from van der Marel et al. (2012).

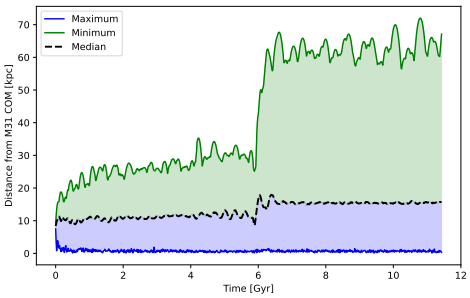

Figure 5. Maximum, minimum, and median radius from Sun-like M31 particles in kpc are plotted on the y-axis against the time in Gyr on the x-axis. In agreement with the video referenced in Figure 4, most particles remain within about 30 kpc of the M31 COM until 6 billion years from today. At this point, the MW and M31 have almost completely merged, and a significant number of candidate stars are cast into streams and have their orbits disrupted. Still, the maximum radius remains bounded below about 75 kpc, meaning that no particles are completely ejected from the system. The conclusion is that all Sun-like systems remain gravitationally bound in this simulation.

This result may be a result of the limited size of the simulation. There may be an exceedingly small, but nonzero probability that some systems of the type considered in this work will be ejected after the MW and M31 collide. However, due to the limited number of particles (945,000 total disk stars for M31) in the simulation in comparison to actual number of stars in the galaxy, it may be that the probability is too low to produce a signal. In addition, the simulation required certain assumptions based on the available observational parameters which may be slightly inaccurate.

6. CONCLUSIONS

The Milky Way galaxy and M31 are expected to merge in approximately 6 Gyr, turbulently casting out stars in stellar streams and tidal tails in the process. Determining how specific stellar populations evolve throughout the merger of these two galaxies can help quantitatively constrain and understand the evolution of interacting galaxies. In this work, I present findings which reveal qualitative and quantitative information about how the distributions of Sun-like stars in M31 and M33 change over the course of the merging event. By exploring this facet of galaxy evolution, our understanding of the dynamics of the Local Group is improved and further insight about the far future of the Solar System is revealed.

In this work, I demonstrate how Sun-like particles in M31 which start off in a narrow annulus in the disk of the galaxy end up spherically distributed throughout the merger remnant. Despite having a drastic change in kinematic properties, these objects all remain gravitationally bound to the system. This result answers a previously unexplored question about the fate of these Sun-like bodies in M31. Along with previous research from van der Marel et al. (2012), which analyzes similar stars in the MW, these results are suggestive of the potential future dynamics of other systems of colliding galaxies of similar sizes to the MW and M31. If this class of objects is distinguishable in other interacting spiral galaxies, they are likely to remain within or near their hosts following major merger events.

Future studies could be conducted to investigate similar phenomena and answer related questions. For example, additional analysis could study whether Sun-like stars from M33 are ejected or remain within the local group after a longer period of time. It is possible that M33 may eventually fall into the merger remnant, which could further alter the kinematics of the system. Other studies could also observe the migration of other classes of stars at other radii, or make selections with other specifications of the criteria regarding the maximum out-of-plane velocity.

Thank you to Professor Gurtina Besla and TA Hayden Foote for instructing the Spring 2023 semester ASTR 400B course at the University of Arizona, for facilitating this project and providing data for the simulation, and for their help completing this work.

Software used in the analysis of data includes the Python programming language (Van Rossum et al. 1995), and several Python software packages. These include the NumPy scientific computing package (Van Der Walt et al. 2011), the Matplotlib plotting package (Hunter 2007), the SciPy scientific computing package (Virtanen et al. 2020), and the Astropy astronomy toolbox package (Robitaille et al. 2013). Additional software used includes the IPython command shell (Pérez & Granger 2007) and the Jupyter Notebook computational notebook software (Kluyver et al. 2016).

REFERENCES

Belokurov, V., Erkal, D., Evans, N. W., Koposov, S. E., & Deason, A. J. 2018, MNRAS, 478, 611, doi: 10.1093/mnras/sty982

Belokurov, V., Zucker, D. B., Evans, N. W., et al. 2006, ApJL, 642, L137, doi: 10.1086/504797

Cox, T. J., & Loeb, A. 2008, MNRAS, 386, 461, doi: 10.1111/j.1365-2966.2008.13048.x

Dubinski, J., Mihos, J. C., & Hernquist, L. 1996, ApJ, 462, 576, doi: 10.1086/177174

Hunter, J. D. 2007, Computing in science & engineering, 9, 90

Kluyver, T., Ragan-Kelley, B., Pérez, F., et al. 2016, in IOS Press (IOS Press), 87–90, doi: 10.3233/978-1-61499-649-1-87

Martin, N. F., Ibata, R. A., Rich, R. M., et al. 2014, ApJ, 787, 19, doi: 10.1088/0004-637X/787/1/19

Pérez, F., & Granger, B. E. 2007, Computing in science & engineering, 9, 21

Pomarède, D., Courtois, H. M., Hoffman, Y., & Tully, R. B. 2017, PASP, 129, 058002, doi: 10.1088/1538-3873/aa5b73

Rector, T. A., Levay, Z. G., Frattare, L. M., Arcand, K. K., & Watzke, M. 2017, PASP, 129, 058007, doi: 10.1088/1538-3873/aa5457

Robitaille, T. P., Tollerud, E. J., Greenfield, P., et al. 2013, Astronomy & Astrophysics, 558, A33

Roškar, R., Debattista, V. P., Quinn, T. R., & Wadsley, J. 2012, MNRAS, 426, 2089, doi: 10.1111/j.1365-2966.2012.21860.x

Sohn, S. T., Anderson, J., & van der Marel, R. P. 2012, ApJ, 753, 7, doi: 10.1088/0004-637X/753/1/7

Sparke, L. S., & Gallagher, John S., I. 2007, Galaxies in the Universe: An Introduction (Cambridge University Press)

Torrey, P., Cox, T. J., Kewley, L., & Hernquist, L. 2012, ApJ, 746, 108, doi: 10.1088/0004-637X/746/1/108

van der Marel, R. P. 2015, in Galaxy Masses as Constraints of Formation Models, ed. M. Cappellari & S. Courteau, Vol. 311, 1–10, doi: 10.1017/S1743921315003294

van der Marel, R. P., Besla, G., Cox, T. J., Sohn, S. T., & Anderson, J. 2012, ApJ, 753, 9, doi: 10.1088/0004-637X/753/1/9

Van Der Walt, S., Colbert, S. C., & Varoquaux, G. 2011, Computing in science & engineering, 13, 22

Van Rossum, G., Drake, F. L., et al. 1995, Python reference manual (Centrum voor Wiskunde en Informatica Amsterdam)

Virtanen, P., Gommers, R., Oliphant, T. E., et al. 2020, Nature methods, 17, 261

Willman, B., & Strader, J. 2012, AJ, 144, 76, doi: 10.1088/0004-6256/144/3/76